Contribution of Dual-tree Complex Wavelet to Three-dimensional Analysis of Pavement Surfaces

Kazuya Tomiyama[1], Yuki Yamaguchi[2] and Kazushi Moriishi[2]

[1]Division of Civil and Environmental Engineering, Kitami Institute of Technology, Japan
[2]Obayashi Road Corporation, Japan
tomiyama@mail.kitami-it.ac.jp, yuki-yamaguchi@obayashi-road.co.jp, kazushi-moriishi@obayashi-road.co.jp

Abstract –

Pavement industries in Japan enhance the application of three-dimensional (3D) modeling as a part of the policy called "i-Construction" which applies 3D point cloud data to pavement works. However, distinctive approaches in terms of signal processing are required in practical applications of 3D point clouds to pavement surfaces. An effective and efficient filtering algorithm is then necessary for the analysis. The purpose of this study is to verify the ability of the dual-tree complex wavelet transform (DTCWT) applied to the 3D point clouds measured for pavement surfaces. Unlike conventional continuous and discrete wavelet transforms, the DTCWT allows nearly shift invariant and directional decomposition in two and higher dimensions with less redundant manners. This study conducts a field experiment at a test site paved with precast concrete blocks for the verification. The result shows that the DTCWT provides superior decomposition algorithm to the discrete wavelet transform by enabling effective filtering based on the directional multiresolution analysis. Finally, the performance of DTCWT is proved for the identification of pavement distress and deformation effectively and reasonably in terms of wavelengths and locations in this study.

Keywords –

Dual-tree complex wavelet; Point cloud; Pavement surface; ICT; i-Construction

1 Introduction

Pavement industries in Japan enhance the application of three-dimensional (3D) modeling as a part of the policy called "i-Construction" which applies 3D point cloud data in design, construction, maintenance, and rehabilitation stages of pavements [1]. An advantage of the i-Construction is capable of improving productivity and quality of pavement works by use of Information and Communication Technologies (ICTs). The use of terrestrial laser scanner (TLS) which is one of the unique applications of i-Construction has been studied in terms of establishing technical standards [1], measurement accuracy [2], and measurement efficiency [3,4]. The demand for 3D measurement has also been increasing in the implementation of area-based pavement management rather than line-based one by detecting localized distress and deformation of pavement surfaces [5-8].

On the other hand, distinctive approaches in terms of signal processing are required in practical applications of 3D point clouds. For example, the approaches include removing unwanted noises [9], generating a reference plane [10], and detecting information of interest [11]. In other words, an effective and efficient filtering algorithm is necessary for the analysis of 3D point clouds measured for pavement surfaces in practice. Various filtering techniques to identify features of a signal have so far been developed with convolution digital filters (CDF) [12], short-time Fourier transform (STFT) [7], continuous wavelet transform (CWT) [13], and discrete wavelet transform (DWT) [14]. However, the CDF needs to design different specifications corresponding to different wavebands of interest. It results in the increase of the number of calculations. The STFT allows the simultaneous identification of wavelengths and locations whereas it requires the stationarity assumption of a signal for the analysis. Unlike the CDF and STFT, the CWT and DWT realize efficient filtering and feature identification in the wavelength and location information simultaneously without the assumption of stationarity [15]. Nevertheless, the calculation redundancies of CWT and the shift variant properties of DWT are still remaining as issues in the decomposition of a signal [15,16]. Against the properties of these methods, the dual-tree complex wavelet transform (DTCWT) has been developed to achieve nearly shift invariant and directional decomposition in two and higher dimensions with less redundant manners [16, 17]. This advantage was applied to a pavement distress analysis based on photographic images [18].

In the light of this background, the purpose of this study is to verify the ability of DTCWT applied to the 3D point cloud rather than photographic images acquired for pavement surfaces. For this purpose, this study conducted a field experiment at a test site paved with precast concrete blocks as an example to verify the diagnostic performance of DTCWT applied to the pavement surfaces.

2 Theory of DTCWT

The basic theory of DTCWT obeys the manner of DWT [15] whereas the DTCWT introduces the concept of complex numbers for the scaling and wavelet functions as same as the Fourier transform [17]. This chapter reviews the theory of DTCWT with describing the difference from DWT. The details can be seen elsewhere [15-17]. Note that when point cloud data of pavement surfaces are defined as function of length, the frequency of cycle per length is called wave number. However, the term frequency is used in this chapter unless otherwise specifically noted.

2.1 DWT

Any finite- energy analog signal $x(t)$ as a function of time or distance t can be decomposed in terms of wavelets $\psi(t)$ and scaling functions $\varphi(t)$ via

$$x(t) = \sum_{n=-\infty}^{\infty} c(n)\varphi(t-n) + \sum_{j=0}^{\infty}\sum_{n=-\infty}^{\infty} d(j,n)2^{\frac{j}{2}}\psi(2^j t - n) \quad (1)$$

The scaling coefficients $c(n)$ and wavelet coefficients $d(j,n)$ are computed by the following equations

$$c(n) = \int_{-\infty}^{\infty} x(t)\varphi(t-n)dt \quad (2)$$

$$d(j,n) = 2^{j/2}\int_{-\infty}^{\infty} x(t)\psi(2^j t - n)dt \quad (3)$$

Where j and n denote the scale factor and the shift parameter corresponding to the frequency content and time/distance, respectively. That is, the DWT transforms an original signal into low-pass "approximation" components via the scaling functions and high-pass "detail" components via the wavelets, which can be seen in the first and second term, respectively, on the right-hand side of Equation (1). With this representation, the DWT allows multiresolution analysis using a fast pyramid algorithm.

However, the DWT lacks the property of shift invariance. As a result, the energy of the wavelet coefficient changes significantly against a small time/distance shift in the phase of an input signal [16]. For instance, Figure 1(a) shows step functions which had offsets longitudinally at an interval of 2 m. The steps can be decomposed into level 2 as shown in Figure 1(b) on the basis of 7th order Symlet wavelet [19]. As can be seen in the figure, the oscillations of steps clearly depend on the location.

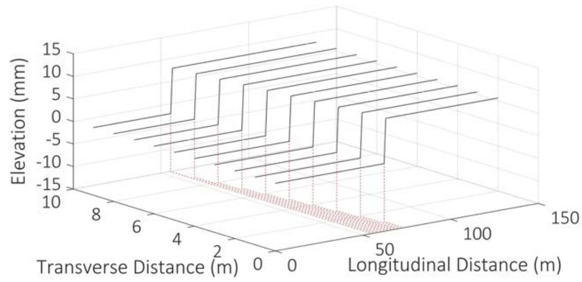

(a) Original Signals

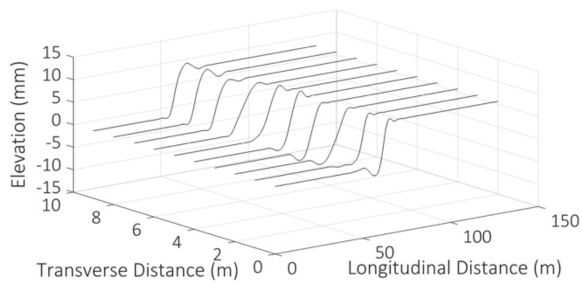

(b) DWT Result

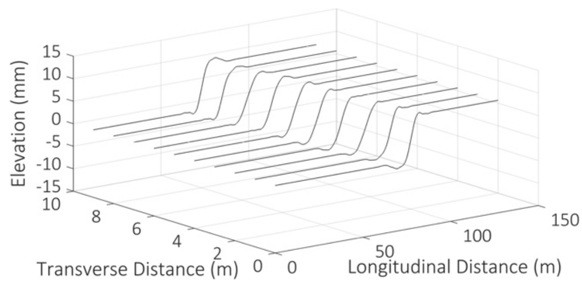

(c) DTCWT Result

Figure 1. Wavelet Analysis Results for Step Functions with Longitudinal Offset

2.2 DTCWT

The signal processing with DTCWT follows that with the DWT shown in Equation (1)-(3). However, the DTCWT involves the concept of complex numbers for the scaling and wavelet functions as same as the Fourier transform [17]. That is, the DTCWT employs complex valued wavelets $\psi_c(t)$ and scaling functions $\varphi_c(t)$ shown in Equation (4) and (5), respectively.

$$\psi_c(t) = \psi_{\mathrm{r}}(t) + \mathbf{i}\psi_{\mathrm{i}}(t) \quad (4)$$

$$\varphi_c(t) = \varphi_{\mathrm{r}}(t) + \mathbf{i}\varphi_{\mathrm{i}}(t) \quad (5)$$

Where **i** denotes the imaginary unit. In Equation (4), $\psi_{\mathrm{r}}(t)$ and $\psi_{\mathrm{i}}(t)$ are the real part and the imaginary part

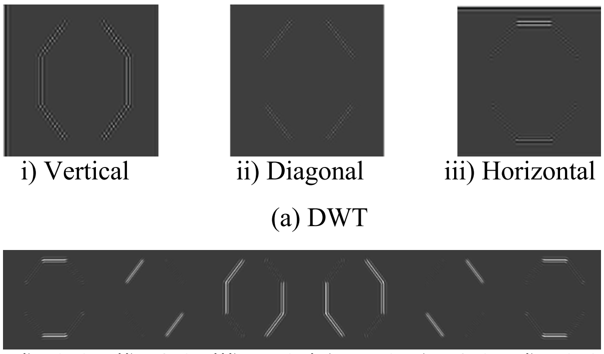

Figure 2. Directional Wavelet Analysis of an Octagon Image

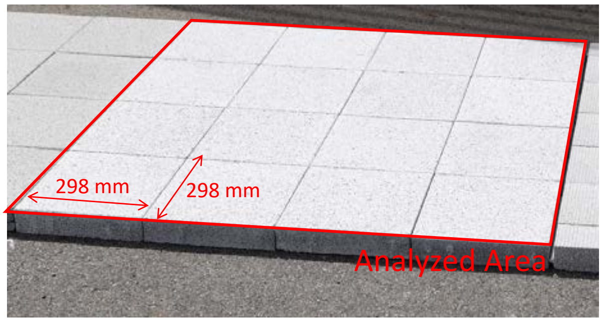

Figure 3. Overview of Target Pavement

Figure 4. TLS (RIEGL VZ-400i)

of the complex wavelet functions, respectively. Here, $\psi_{\mathrm{r}}(t)$ and $\psi_{\mathrm{i}}(t)$ are Hilbert transform pair to each other which is supported on only a Nyquist frequency range. Same is true for the complex scaling functions shown in Equation (5). The complex wavelet coefficient and the magnitude can be computed by Equation (6) and (7), respectively.

$$d_c(j,n) = d_{\mathrm{r}}(j,n) + \mathbf{i}d_{\mathrm{i}}(j,n) \tag{6}$$

$$|d_c(j,n)| = \sqrt{[d_{\mathrm{r}}(j,n)]^2 + [d_{\mathrm{i}}(j,n)]^2} \tag{7}$$

In practice, the DTCWT can be simply implemented with two real DWTs: the first DWT gives the real part of the transform while the second DWT gives the imaginary part [17]. Figure 1(c) indicates the result of level 2 DTCWT with a filter bank based on 9/7 biorthogonal wavelet [20] applied to Figure 1(a). As shown in the figure, the effect of shift variance obviously decreased in comparison with the result of DWT shown in Figure 1(b).

2.3 Directional Analysis

When the transform is expanded in multi-dimensions, the DTCWT performs directional decomposition toward the angles of $\pm 15°$, $\pm 45°$, and $\pm 75°$. This ability allows analyzing and processing oriented singularities such as edges, joints and unevenness in 3D pavement surfaces [17]. Although the DWT is possible to directional decomposition toward the horizontal ($\pm 0°$), diagonal ($\pm 45°$), and vertical ($\pm 90°$) directions, it brings the aliasing for the diagonal orientations.

Figure 2 illustrates the level 3 decomposition of an octagon image by the DWT and DTCWT. As shown in the figures, the DWT produces a checkerboard artifact on the diagonal orientation whereas the result obtained with DTCWT is free of it. The directional decomposition result of DTCWT can be reconstructed for any combinations of orientations. The applicability of this performance to a 3D measured pavement surface is described in the rest of this paper.

3 Verification Field Experiment

A field experiment was conducted to verify the diagnostic performance of DTCWT applied to the pavement surfaces. The target surface was paved with precast concrete blocks as shown in Figure 3. The point clouds were acquired with a TLS (RIEGL VZ-400i) shown in Figure 4.

3.1 Pre-processing of Point Clouds

As a pre-processing, measured data are rotated to obey the mathematical coordinate system for exploiting the directional performance of DTCWT. Then, since the density of point clouds depends on the distance from the TLS to the target object, intervals between each point are resampled to be a constant value according to the purpose of analysis. In this study, a constant interval of 1 mm is set in respect to the interaction between surface properties and micromobilities [21]. Figure 5(a) shows the contour map of measured point clouds after the pre-processing. At a glance, only a slope from the top left to bottom right can be observed in the figure whereas no diagnostic findings in terms of pavement surface characteristics are recognized.

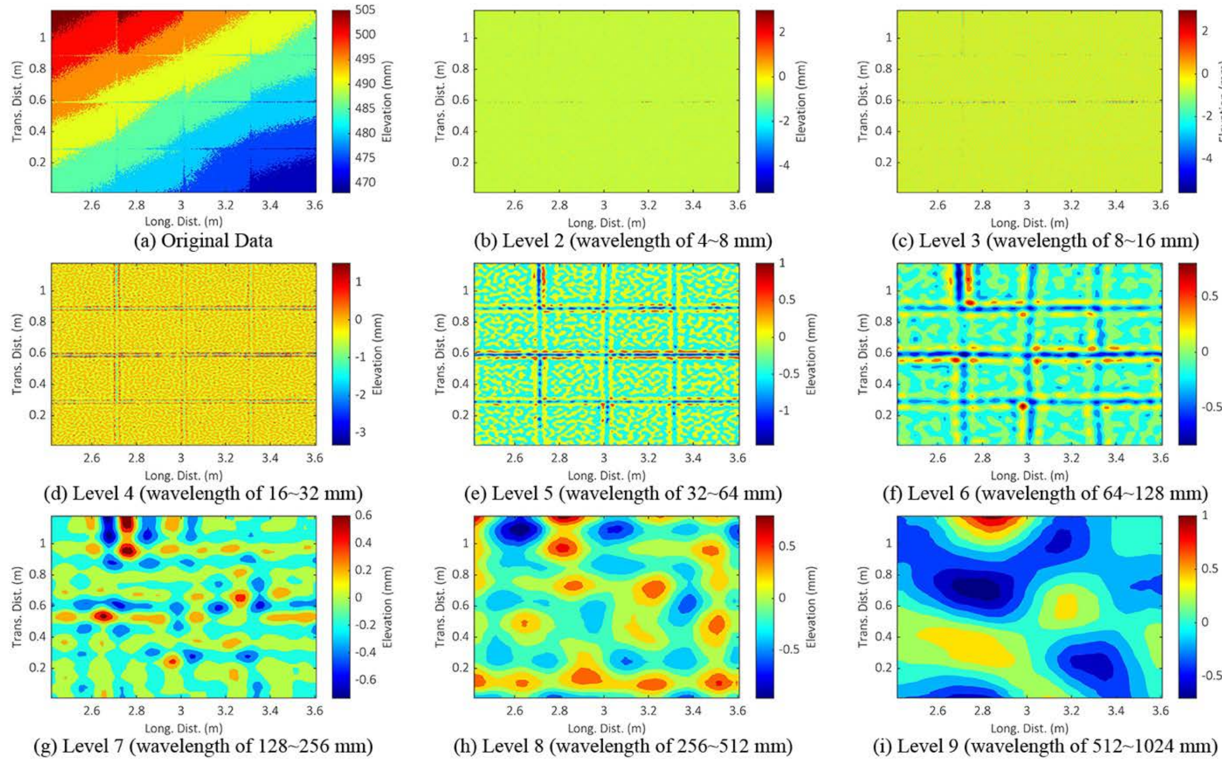

(a) Original Data (b) Level 2 (wavelength of 4~8 mm) (c) Level 3 (wavelength of 8~16 mm)
(d) Level 4 (wavelength of 16~32 mm) (e) Level 5 (wavelength of 32~64 mm) (f) Level 6 (wavelength of 64~128 mm)
(g) Level 7 (wavelength of 128~256 mm) (h) Level 8 (wavelength of 256~512 mm) (i) Level 9 (wavelength of 512~1024 mm)

Figure 5. Multiresolution Analysis of Block Pavement

3.2 Result of Multiresolution Analysis

The DTCWT performs a multiresolution analysis by decomposing an original signal into low-pass approximation and high-pass detail components The approximation component is further decomposed repeatedly with the same manner. This technique contributes to the diagnosis of pavement surface characteristics in terms of the simultaneous identification of wavelengths and locations.

Figure 5 indicates the result of omnidirectional multiresolution analysis from level 2 to 9 without the direct current component for the measured pavement surface. Here, the result of level 1 is excluded because no meaningful information is detected. As shown in the figure, the result provides diagnostic viewpoints based on the decomposition levels as follows:

- Level 4 component depicts the edge deterioration of precast concrete blocks,
- Level 5 to 6 components emphasize the localized joint faults, and
- Level 7 to 9 components illustrate the unevenness of the surface due mainly to the irregularity of base course.

When a practical application that identifies blocks deviated vertically is considered, level 4 highlighting edge locations and level 7 to 9 associated with unevenness can be integrated by the reconstruction of wavelets as shown in Figure 6. As shown in the figure, the severe vertical displacement of a block located at the first row of the second column from the top left can be identified. This result demonstrates that the DTCWT achieves the effective vis-

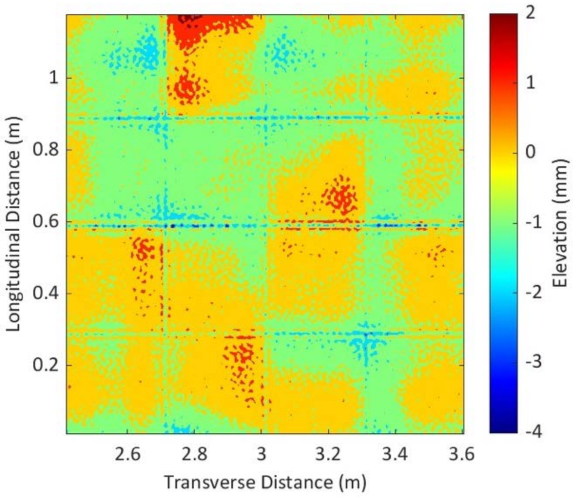

Figure 6. Reconstruction of Specific Levels Associated with Edge and Unevenness Components

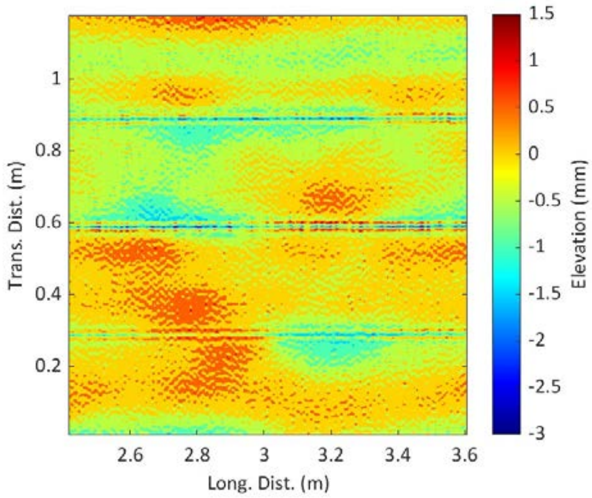

(a) Transverse Direction

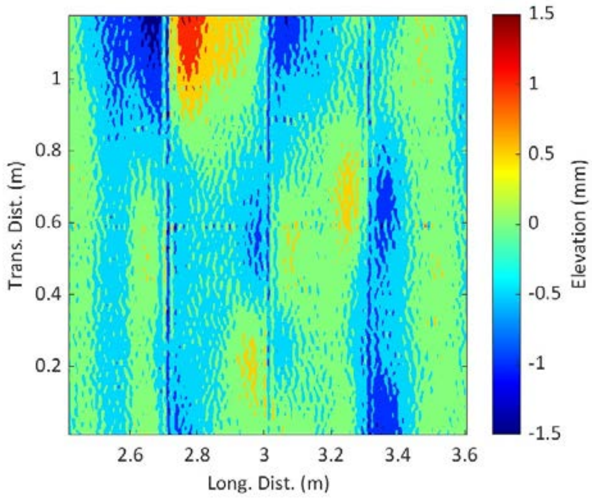

(b) Longitudinal Direction

Figure 7. Result of Directional Multiresolution Analysis

ualization and evaluation of pavement distress and deformation considering wavelengths and locations.

3.3 Directional Multiresolution Analysis

A distinctive ability of DTCWT realizes a directional multiresolution analysis of 3D point clouds It allows the recognition of orientation and spread of pavement distress and deformation. Figure 7 shows the result of directional multiresolution analysis for the target pavement. Here the longitudinal direction is defined with a combination of the orientations at ±75° whereas the transverse direction consists of a combination between the orientation at ±15° and ±45°.

According to Figure 7, the deviation of the block identified in the previous section mostly occurs at the longitudinal direction. This fact corresponds visually to the actual situation of the site. Thus, the longitudinal correction of the base course needs to be planed as a possible rehabilitation activity of the pavement.

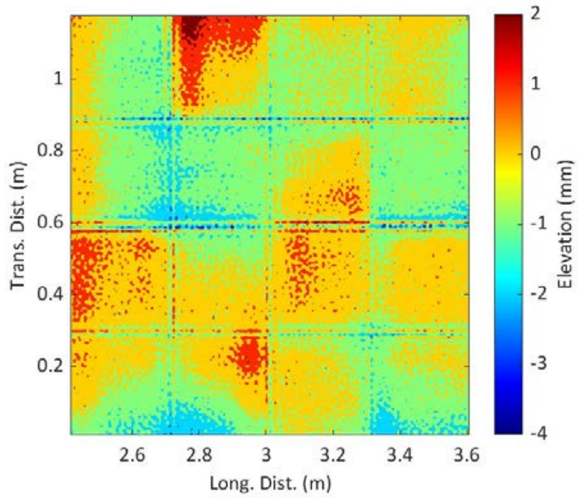

Figure 8. Reconstruction of Specific Levels Associated with Edge and Unevenness Components

3.4 Comparison with Conventional DWT

As theoretically described above, the DTCWT overcomes the shortcomings of conventional DWT in terms of the shift variant properties. This section performs the DWT for the same measured pavement surface. Figure 8 shows the reconstruction result based on the DWT in the same manner of Figure 6. As shown in Figure 8, trivial differences with Figure 6 are observed at first glance. Here, note that the result of DWT is shift variant and suffers from aliasing effects in diagonal orientation components. Figure 9 and Figure 10 show the oriented DWT and DTCWT, respectively. As shown in the figures, checkerboard artifacts due to aliasing effects can be apparently seen in the diagonal components of DWT unlike the result of DTCWT. The artifact leads to misinterpretation on the inspection result of pavement surfaces. Consequently, the capability of the directional multiresolution analysis with the DTCWT contributes to providing the evidence for the reasonable decision on pavement maintenance and rehabilitation activities.

4 Discussion and Conclusions

The pavement engineering fields nowadays widely attempts to apply 3D measurement technologies against the demand for improving construction quality as well as the productivity. However, the effective use of 3D data is still challenging due to the requirement of distinctive

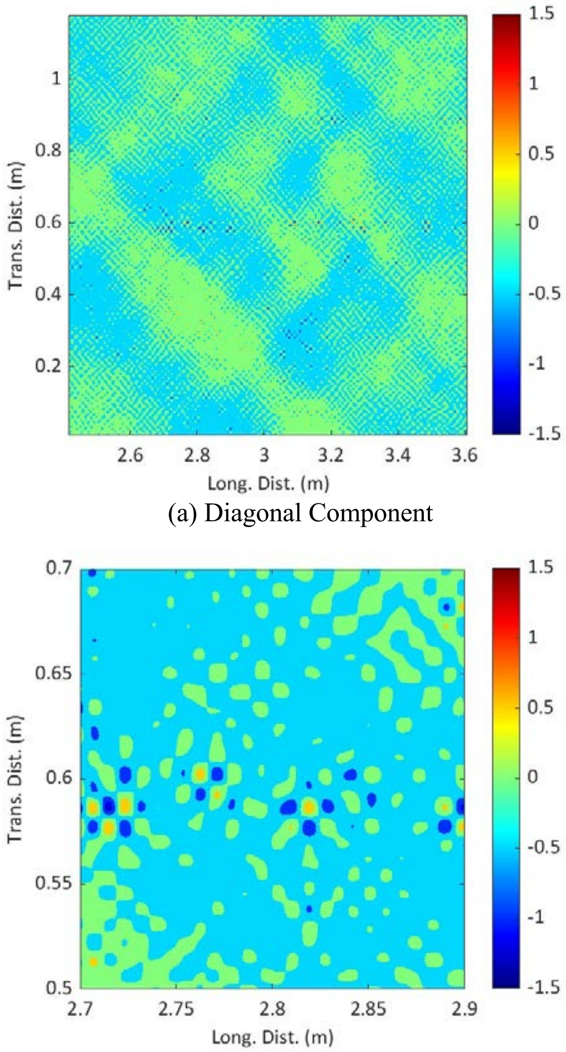

(a) Diagonal Component

(b) Detail

Figure 9. An Example of Oriented DWT

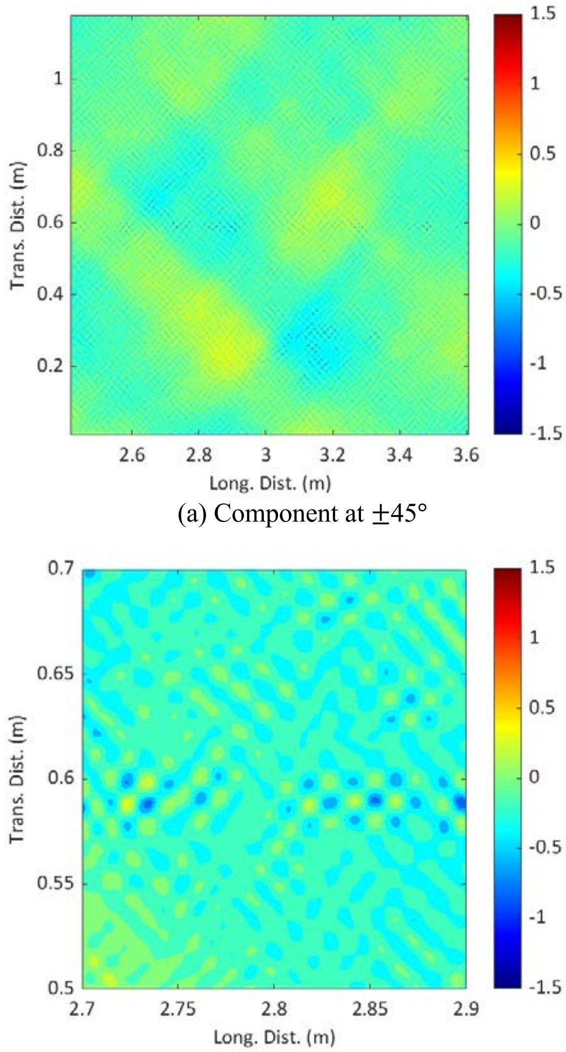

(a) Component at ±45°

(b) Detail

Figure 10. An Example of Oriented DTCWT

analysis techniques apart from conventional 2D-based methods. In the light of this background, this study has introduced a novel approach applying the DTC WT to 3D measured pavement surfaces. The DTCWT overcomes the shortcomings of conventional DWT by introducing the imaginary part in wavelet and scaling functions. The performance of DTCWT allows the effective filtering to identify pavement distress and deformation based on the directional multiresolution analysis. This study has validated the capability of the DTCWT in pavement surface analysis.

In this study, a field experiment which was subject to the pavement with precast concrete blocks was conducted to prove the capability of DTCWT. Although the measured original data provided no diagnostic findings in terms of the pavement surface characteristics, the multiresolution analysis based on the DTCWT emphasized the specific wavelengths and locations related to the edge, joint, and unevenness. Consequently, the performance of DTCWT has been demonstrated for the effective visualization and evaluation of pavement distress and deformation.

This study also described the directional multiresolution analysis of 3D point clouds as a unique ability of DTCWT. As a result, the DTCWT was able to identify the orientation and spread of distress and deformation in the measured pavement. The advantage of DTCWT over DWT in terms of the oriented transform was validated as well. Finally, this study concluded that the directional multiresolution analysis with the DTCWT provides the evidence for the reasonable decision on pavement maintenance and rehabilitation activities.

According to the findings acquired with this study, the performance of DTCWT has been proved for the analysis of 3D point clouds effectively and reasonably in terms of the data filtering.

References

[1] Kondo, K., Morikawa, H., Masuta, Y., Yamaguchi, A., Takemoto, N., and Kumamoto, Y. New Standard for Dimensional Control with Lider in Public Pavement Work, *Journal of Japan Society of Civil Engineers, Ser. F3 (Civil Engineering Informatics)*, 73 (2), pages I_83-I_91, 2017.

[2] Higuchi, T., Sada, T., Emori, H., Murayama, S., and Fukumori, H. Study on the Mesurement Finished Shapes by TLS in Pavement Work, *Journal of Japan Society of Civil Engineers, Ser. F3 (Civil Engineering Informatics)*, 75 (2), Pages II_71-II_78, 2019.

[3] Moriishi, K. and Tomiyama, K. Efficient Improvement of Point Cloud Data Acquisition and Expansion of Application Fields into ICT Pavement Construction, *Journal of Japan Society of Civil Engineers, Ser. E1 (Pavement Engineering)*, 75 (2), Pages I_77-I_85, 2019.

[4] Moriishi, K., Tomiyama, K, Nishikawa, K., and Yamaguchi, Y. Improvement of Operational Efficiency on Road Surface Control using 3-D Measurement Devices, *Journal of Japan Society of Civil Engineers, Ser. E1 (Pavement Engineering)*, 76 (2), Pages I_169-I_177, 2020.

[5] Moriishi, K. Nakamura, H., and Watanabe, K. A Study of the New Road Surface Evaluation Method using Three-Dimensional Coordinate Data, *Journal of Japan Society of Civil Engineers, Ser. E1 (Pavement Engineering)*, 69 (3), Pages I_9-I_16, 2013.

[6] Eguchi, M., Kawamura, A., Tomiyama, S., Takahashi, S., and Endo, K. A Basic Study on Evaluation of Spotted Surface Defects by a 3-dimension Formulating System using Transverse Profile Data, *Journal of Japan Society of Civil Engineers, Ser. E1 (Pavement Engineering)*, 73 (3), Pages I_71-I_78, 2017.

[7] Hirano, H., Mizutani, T., Ishida, T., Annaka, S., and Suzuki, K. Evaluation of Local Deterioration of Pavement Surface by Spatial Frequency Analysis based on Short-Time Fourier Transform, Journal of Japan Society of Civil Engineers, Ser. E1 (Pavement Engineering), 74 (3), Pages I_113-I_120, 2018.

[8] Eguchi, M., Kawamura, A., Tomiyama, K., and Omachi, S. A Simplified Method of Detecting Spot Surface Defects by using Quasi-3D Data from a Conventional Road Profiler, *Transportation Research Record*, 2673 (11), pages. 1-11, 2019.

[9] Han, X.F., Jin, S.J., Wang, M., Jiang, W., Gao, L., and Xiao, L. A Review of Algorithms for Filtering the 3D Point Cloud, *Signal Processing: Image Communication*, 57, pages103-112, 2017.

[10] Liang, J., Gu, X., Chen, Y., Ni, F., and Zhang, T. A Novel Pavement Mean Texture Depth Evaluation Strategy based on Three-dimensional Pavement Data Filtered by a New Filtering Approach, *Measurement*, 166 (108265), 2020.

[11] PIARC. Optimization of Surface Characteristics, Technical Committee Report on Surface Characteristics, *Technical Committee Report on Surface Characteristics*, pages 13-19, PIARC Xviii World Road Congress, 1987.

[12] Deng, Q., Zhan, Y., Liu, C., Qiu, Y., and Zhang, A. Multiscale Power Spectrum Analysis of 3D Surface Texture for Prediction of Asphalt Pavement Friction, *Construction and Building Materials*, 293 (123506), 2021.

[13] Puri, N., Valero, E., Turkan, Y., and Bosché, F. Assessment of Compliance of Dimensional Tolerances in Concrete Slabs using TLS Data and the 2D Continuous Wavelet Transform, *Automation in Construction*, 94, pages 62-72, 2018.

[14] Parrish, C. Exploiting Full-Waveform Lidar Data and Multiresolution Wavelet Analysis for Vertical Object Detection and Recognition, *IEEE International Geoscience and Remote Sensing Symposium (IGARSS)*, 420, 2007.

[15] Mallat, S. *Wavelet Tour of Signal Processing*, Academic Press, New York, 1999.

[16] Kingsbury, N. Complex Wavelets for Shift Invariant Analysis and Filtering of Signals, *Applied and Computational Harmonic Analysis*, 10 (3), pages 234-253, 2001.

[17] Selesnick, I.W., Baraniuk, R.G., and Kingsbury, N.C. The Dual-tree Complex Wavelet Transform, *IEEE Signal Processing Magazine*, 22 (6), pages 123-151, 2005.

[18] Wang, J. and Gao, R., Pavement Distress Analysis based on Dual-Tree Complex Wavelet Transform, *International Journal of Pavement Research and Technology*, 5 (5), pages 283-288, 2012.

[19] Daubechies, I. *Ten Lectures on Wavelets*, Society for Industrial and Applied Mathematics, 1992.

[20] Antonini, M., Barlaud, M., Mathieu, P., and Daubechies, I., Image Coding Using Wavelet Transform, *IEEE Transactions on Image Processing*, 1 (2), pages 205-220, 1992.

[21] Tomiyama, K. and Moriishi, K. Pavement Surface Evaluation Interacting Vibration Characteristics of an Electric Mobility Scooter, *Lecture Notes in Civil Engineering*, 76, pages 893-900, 2020.